

SLAC-PUB-5335
September 1990
(T/E)

SEMILEPTONIC BARYON DECAYS WITH A HEAVY QUARK^{*}

ROBERT SINGLETON JR.

*Stanford Linear Accelerator Center
Stanford University, Stanford, California 94309*

ABSTRACT

The semileptonic decay of spin-1/2 baryons is examined in the spectator quark-model, with special attention given to $\Lambda_b \rightarrow \Lambda_c e \nu$ and $\Omega_b \rightarrow \Omega_c e \nu$. The polarization of the virtual- W and of the daughter baryon is also considered, along with the joint angular distribution between the charged lepton and the daughter baryon polarization vector. The Λ_b decays with about equal mixtures of transverse- to longitudinal- W polarization while the Ω_b decays with predominately longitudinal- W polarization. These reactions are representative of two qualitatively different classes: decays involving baryons whose spectators are spin-singlets and those whose spectators are spin-triplets.

Submitted to *Physical Review D*

^{*} Work supported by Department of Energy contract DE-AC03-76SF00515.

1. Introduction

There has been much effort lately in calculating semileptonic decays of mesons. Eventually one hopes to extract the KM-mixing angles and probe the quark structure of hadrons. The quark model has been reasonably successful in describing both inclusive¹⁹ and exclusive processes.²⁻⁵ These calculations agree quite well for decays like $D^+ \rightarrow K^0 e^+ \nu_e$ and $B \rightarrow D^* e^+ \nu$, and they even predict the correct longitudinal to transverse D^* ratio. If these calculations are in fact reliable, and give accurate values for the form factors, then Kobayashi-Maskawa matrix elements may be extracted.

Last year, however, a serious discrepancy between the quark model and experiment arose in the decay of charmed mesons. Both the rate and the polarization ratio in the $D \rightarrow K^* e^+ \nu_e$ calculation are in conflict with experiment. The calculation^{2,3} predicts comparable $D \rightarrow K^* e^+ \nu_e$ and $D \rightarrow K e^+ \nu_e$ rates and about equal longitudinal and transverse production of K^* final states. The experiment⁶ shows, however, that the rate for $D \rightarrow K^* e^+ \nu_e$ is about half that for $D \rightarrow K e^+ \nu_e$, and that K^* final states are predominantly longitudinal.

This has inspired several attempts to re-examine the quark model and the underlying assumptions involved in the calculations.⁷⁻⁹ Although *ad hoc* adjustments of form factors can be made to fit the data,¹⁰ there is no compelling *theoretical* motivation for doing this. In many of the models considered, a nonrelativistic approach was adopted. While this could be justified for heavy quarks, it is dubious for the light spectators. It is important to know whether the failure of the quark model might simply be relativistic effects that have not been considered, or something more fundamental. It is a little puzzling, however, if the failure is just due to relativistic effects. The K^* system is less relativistic than the K system, so naively one should expect even better agreement with experiment for $D \rightarrow K^* e^+ \nu_e$ than for $D \rightarrow K e^+ \nu$. However, there is an important difference— $D \rightarrow K^* e^+ \nu_e$ involves a quark-spin flip while $D \rightarrow K e^+ \nu_e$ does not—and this might be enough to substantially change the wave function from the naive quark model form.

It is important to study other hadronic systems and see how the quark model fares. The strongly stable baryons are ideal for this, and data should soon be available. In this paper I give special attention to the semileptonic decays of Λ_Q and Ω_Q for $Q = b, c$. For completeness I also present results for Σ_Q and Ξ_Q . The angular distribution of the charged lepton and the polarization of the virtual W is examined. I also give the joint angular distribution between the charged lepton and the daughter baryon polarization vector. This should provide enough information to determine the helicity form factors independently, which may indicate where the quark model might be breaking down, if in fact it does.

2. Kinematics

This paper examines exclusive semi-leptonic decays of spin-1/2 baryons and in particular the angular distribution of the charged lepton, which I take to be a massless electron. Much of this section is a standard exercise; it is presented elsewhere^{11,12,10} and is repeated here for completeness and to establish notation.

Figure 1 shows this process for a parent baryon with a generic heavy quark Q that decays into a baryon with a lighter, but still relatively heavy, quark q . For the process $M \rightarrow me\bar{\nu}$ the decay rate is given by

$$d\Gamma(M_s \rightarrow m_{s'}e\bar{\nu}) = \frac{1}{2M} |A(M_s \rightarrow m_{s'}e\bar{\nu})|^2 d\Pi_3, \quad (2.1)$$

where

$$d\Pi_3 = (2\pi)^4 \delta^{(4)}(P - k - p - p') \prod_f \frac{d^3\mathbf{k}_f}{(2\pi)^3 2E_f}, \quad (2.2)$$

and

$$A(M_s \rightarrow m_{s'}e\bar{\nu}) = \frac{G_F}{\sqrt{2}} V_{Qq} L^\mu H_\mu^{(s's)}, \quad (2.3)$$

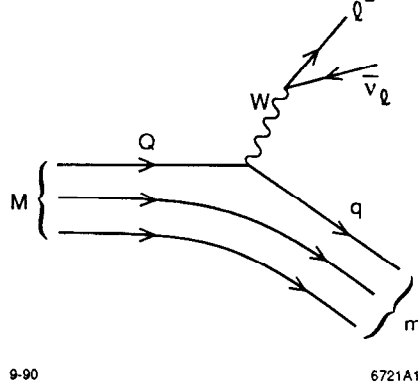


Fig. 1. The semileptonic decay of a heavy quark Q into a lighter quark q and a virtual W , which becomes a charged lepton and neutrino.

with V_{Qq} being the Kobayashi-Maskawa matrix element appropriate to the $Q \rightarrow q$ transition and where the product is over all final-state momenta. I am using a somewhat redundant notation where $M_s(m_{s'})$ refers to the parent (daughter) baryon of mass $M(m)$ and spin component $s(s')$. The parent has four-momentum P , the daughter k , the e and $\bar{\nu}$ have p and p' respectively. The virtual W carries four-momentum $q = p + p'$. It should be kept in mind that the spin-quantization axes for the parent and daughter baryons are not necessarily chosen the same.

The leptonic and hadronic currents are given by

$$L^\mu = \bar{u}_e \gamma^\mu (1 - \gamma_5) v_\nu, \quad (2.4)$$

$$H^{(s's)\mu} = \langle k, s' | J_{had}^\mu(0) | P, s \rangle. \quad (2.5)$$

If the final state leptons are $e^+ \nu$ instead, the order of the spinors in the lepton current must be changed. The hadronic current can be constructed from Lorentz invariant form factors and the four-vectors of the problem. Writing $J_{had}^\mu = V^\mu - A^\mu$, I define

$$\begin{aligned} \langle k | V^\mu(0) | P \rangle = & \bar{u}_m [g(q^2) \gamma^\mu + g_+(q^2)(P + k)^\mu \\ & + g_-(q^2)(P - k)^\mu] u_M, \end{aligned} \quad (2.6)$$

$$\begin{aligned} \langle k | A^\mu(0) | P \rangle = & \bar{u}_m [a(q^2)\gamma^\mu\gamma_5 + a_+(q^2)(P+k)^\mu\gamma_5 \\ & + a_-(q^2)(P-k)^\mu\gamma_5] u_M, \end{aligned} \quad (2.7)$$

where $q^2 = (P - k)^2$ and u_M (u_m) is the spinor associated with the parent (daughter) baryon and spin labels have been suppressed. It is convenient to use dimensionless kinematic variables $y = q^2/M^2$ and $x = P \cdot p/M^2$, scaling to the parent baryon mass. Neglecting the mass of the electron, the kinematically allowed limits of y are from 0 to $(1 - m/M)^2$.

In the parent rest frame I denote quantities by a tilde, and reserve the notation E_e , E_m , etc., without the tilde, for quantities in the $e\bar{\nu}$ center-of-mass frame ($e\bar{\nu}$ frame) where the amplitude will turn out to have a simple angular dependence. Let $-\tilde{\mathbf{k}}$ define the direction of the positive z axis and let θ_e be the angle of the electron relative to this axis in the $e\bar{\nu}$ frame, with the y axis oriented perpendicular to the decay plane defined by the m , e , and $\bar{\nu}$ momenta, as shown in Fig. 2(a) (note that \mathbf{k} and $\tilde{\mathbf{k}}$ are anti-parallel). In the $e\bar{\nu}$ frame the natural variables are the electron energy,

$$E_e = E_\nu = \frac{M}{2}\sqrt{y}, \quad (2.8)$$

and $\cos\theta_e$. On the other hand, in the parent rest frame the natural variables are

$$\tilde{E}_e = Mx \quad (2.9)$$

and $y = q^2/M^2$.

The mass-shell relation $P^2 = (q + k)^2 = M^2$ may be used to obtain expressions for the energy and momentum of the parent and daughter baryons, respectively:

$$E_M = \frac{M}{2\sqrt{y}} \left[1 - \frac{m^2}{M^2} + y \right], \quad (2.10)$$

$$E_m = \frac{M}{2\sqrt{y}} \left[1 - \frac{m^2}{M^2} - y \right], \quad (2.11)$$

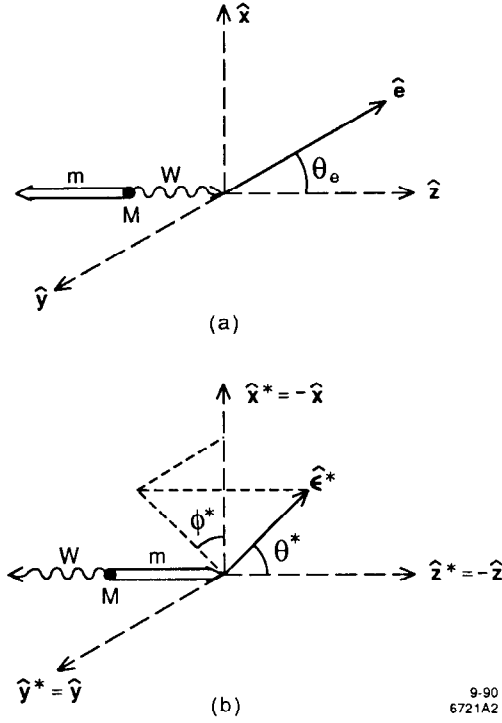


Fig. 2. Coordinate system for semileptonic decay of a heavy baryon: (a) the decaying virtual W and (b) the decaying daughter baryon.

and

$$|\mathbf{P}| = |\mathbf{k}| = K/\sqrt{y} \quad (2.12)$$

in the $e\bar{\nu}$ frame; whereas in the parent rest frame

$$\tilde{E}_m = \frac{M}{2} \left[1 + \frac{m^2}{M^2} - y \right], \quad (2.13)$$

and

$$|\tilde{\mathbf{k}}| = K, \quad (2.14)$$

where

$$K \equiv \frac{M}{2} \left[\left(1 - \frac{m^2}{M^2} - y \right)^2 - 4 \frac{m^2}{M^2} y \right]^{1/2}. \quad (2.15)$$

The connection between the natural variables in the two frames is made complete by expressing the angular variable in the $e\bar{\nu}$ frame, $\cos\theta_e = -\cos\theta_\nu$, in terms of variables in the parent rest frame and evaluating $P \cdot p$ in the two frames; one finds

$$Mx = \tilde{E}_e = \frac{K}{2} \cos\theta_e + \frac{M}{4} \left[1 - \frac{m^2}{M^2} + y \right]. \quad (2.16)$$

The Feynman amplitude is Lorentz invariant and it is convenient to split the phase space into Lorentz-invariant pieces so that it takes a particularly simple form:

$$d\Pi_3 = \frac{M}{(4\pi)^5} K dy d\Omega_e d\tilde{\Omega}_m, \quad (2.17)$$

where $d\Omega_e$ is the solid angle of the electron in the $e\bar{\nu}$ frame and $d\tilde{\Omega}_m$ is the solid angle of the final baryon in the parent rest frame. This gives the differential decay rate:

$$\frac{d\Gamma_{s's}}{dy d\Omega_e d\tilde{\Omega}_m} = \frac{1}{2} \frac{K}{(4\pi)^5} |A_{s's}|^2, \quad (2.18)$$

where the baryon spin dependence is emphasized.

The amplitude in the $e\bar{\nu}$ frame becomes, after summing over electron and neutrino spins,

$$|A_{s's}|^2 \equiv |A(M_s \rightarrow m_{s'} e\bar{\nu})|^2 = \frac{G_F^2}{2} |V_{qQ}|^2 L^{\mu\nu} H_\mu^{(s's)} H_\nu^{(s's)\dagger}, \quad (2.19)$$

and for a massless electron the only non-zero components of the lepton tensor are spatial:

$$L^{ij} = 4M^2 y [(\delta^{ij} - \hat{\mathbf{e}}^i \hat{\mathbf{e}}^j) - i\eta \epsilon^{ijk} \hat{\mathbf{e}}^k], \quad (2.20)$$

where $\eta = +1$ for $e\bar{\nu}$ and $\eta = -1$ for $e^+\nu$ final lepton states and $\hat{\mathbf{e}}$ is a unit vector along the charged-lepton direction in the $e\bar{\nu}$ frame.

It is useful to expand the spatial components of the hadronic current in terms of a helicity basis (effectively that of the virtual W):

$$\mathbf{H}^{(s's)} = H_+^{(s's)} \hat{\mathbf{e}}_+ + H_-^{(s's)} \hat{\mathbf{e}}_- + H_0^{(s's)} \hat{\mathbf{e}}_0, \quad (2.21)$$

where $\hat{e}_\pm = \frac{1}{\sqrt{2}}(\mp\hat{x} - i\hat{y})$ and $\hat{e}_0 = \hat{z}$. Putting Eqs. (2.20) and (2.21) into Eq. (2.19) gives

$$\begin{aligned}
|A_{s's}|^2 = & \frac{G_F^2}{2} |V_{qq}|^2 4M^2 y \left[\frac{1}{2}(1 - \eta \cos \theta_e)^2 |H_+|^2 + \frac{1}{2}(1 + \eta \cos \theta_e)^2 |H_-|^2 \right. \\
& + \sin^2 \theta_e |H_0|^2 + \frac{1}{2} \sin^2 \theta_e (H_+ H_-^* + H_+^* H_-) \\
& - \frac{\eta}{\sqrt{2}} \sin \theta_e (1 - \eta \cos \theta_e) (H_+ H_0^* + H_+^* H_0) \\
& \left. - \frac{\eta}{\sqrt{2}} \sin \theta_e (1 + \eta \cos \theta_e) (H_- H_0^* + H_-^* H_0) \right]. \quad (2.22)
\end{aligned}$$

The angular dependence in this equation is entirely a reflection of the $V - A$ character of the $W \rightarrow e\nu$ amplitude. The baryon spin-sums have not yet been performed and the spin-dependence of the helicity amplitudes, $H_{\pm,0}^{(s's)}$, has been suppressed. When spin is to be emphasized, daughter and then parent spins are listed. I will average over the parent spins, which will be taken along the z -axis; however, I will at first consider the daughter polarization along an arbitrary direction \hat{e} . Since the parent and daughter are back-to-back in the $e\bar{\nu}$ frame, a positive-helicity daughter corresponds to spin-up along $-z$. It is then better to express \hat{e} in terms of polar and azimuthal angles, θ^* and ϕ^* , in the helicity frame shown in Fig. 2(b).¹³

It remains to relate the helicity amplitudes $H_{\pm,0}^{(s's)}$ to the form factors defined in Eqs. (2.6) and (2.7). I normalize the spinors so that $\bar{u}u = 1$ and use the γ -matrix conventions of Ref. 14. Letting ϕ_s and χ_s be two component Pauli-spinors along z and \hat{e} respectively, a short calculation gives the spatial components of the current in the $e\bar{\nu}$ frame as

$$\mathbf{V}^{(s's)} = \chi_{s'}^\dagger \left[-(2kg_+ F_0 + gF_+) \hat{e}_0 - igF_- \hat{\sigma} \times \hat{e}_0 \right] \phi_s, \quad (2.23)$$

$$\mathbf{A}^{(s's)} = \chi_{s'} \left[aF_0 \hat{\sigma} + [2a(1 - F_0) - 2ka_+ F_-] (\hat{\sigma} \cdot \hat{e}_0) \hat{e}_0 \right] \phi_s, \quad (2.24)$$

where

$$F_{\pm} \equiv \left[\frac{(E_m + m)(E_M + M)}{4Mm} \right]^{1/2} \left[\frac{k}{E_m + m} \pm \frac{k}{E_M + M} \right], \quad (2.25)$$

$$F_0 \equiv \left[\frac{(E_m + m)(E_M + M)}{4Mm} \right]^{1/2} \left[1 - \frac{k^2}{(E_m + m)(E_M + M)} \right], \quad (2.26)$$

with $\mathbf{k} = -k\mathbf{e}_0$, and k given by Eq. (2.12). Explicitly, $\mathbf{H}^{(s's)} = \mathbf{V}^{(s's)} - \mathbf{A}^{(s's)}$ gives¹⁵

$$\mathbf{H}^{(\pm\pm)} = -\sqrt{2} h_{\mp} e^{\mp i\phi^*/2} \sin \frac{\theta^*}{2} \hat{\mathbf{e}}_0 \pm \sqrt{2} H_{\pm} e^{\pm i\phi^*/2} \cos \frac{\theta^*}{2} \hat{\mathbf{e}}_{\pm}, \quad (2.27)$$

$$\mathbf{H}^{(\pm\mp)} = -\sqrt{2} H_{\mp} e^{\mp i\phi^*/2} \sin \frac{\theta^*}{2} \hat{\mathbf{e}}_{\mp} \pm \sqrt{2} h_{\pm} e^{\pm i\phi^*/2} \cos \frac{\theta^*}{2} \hat{\mathbf{e}}_0, \quad (2.28)$$

where

$$H_{\pm} \equiv \pm [aF_0 \mp gF_{-}], \quad (2.29)$$

$$h_{\pm} \equiv \pm \frac{1}{\sqrt{2}} \left[2a \left(1 - \frac{1}{2}F_0 \right) - 2ka_+F_{-} \mp (2kg_+F_0 + gF_+) \right]. \quad (2.30)$$

Comparison with Eq. (2.21) gives $H_{\pm,0}^{(s's)}$. When $\hat{\mathbf{e}} = -\hat{\mathbf{e}}_0$ the spin and helicity of the daughter particle are the same. Notice that $(s's) = (\pm\pm)$ produces purely transverse W s while $(s's) = (\pm\mp)$ produces purely longitudinal W s. Using Eq. (2.18) and averaging over the initial spin gives the rate:

$$\begin{aligned} \frac{d\Gamma_{s'}}{dy d\Omega_e d\tilde{\Omega}_m} &= \frac{G_F^2 |V_{qq}|^2 KM^2 y}{(4\pi)^5} \left\{ \frac{1}{2} (1 - \eta \cos \theta_e)^2 \left(\frac{1 + s' \cos \theta^*}{2} \right) |H_+|^2 \right. \\ &+ \frac{1}{2} (1 + \eta \cos \theta_e)^2 \left(\frac{1 - s' \cos \theta^*}{2} \right) |H_-|^2 \\ &+ \left[|h_-|^2 \left(\frac{1 - s' \cos \theta^*}{2} \right) + |h_+|^2 \left(\frac{1 + s' \cos \theta^*}{2} \right) \right] \sin^2 \theta_e \\ &+ \frac{\eta s'}{\sqrt{2}} [\sin \theta_e (1 - \eta \cos \theta_e) (\cos \phi^* \sin \theta^*)] H_+ h_- \\ &\left. + \frac{\eta s'}{\sqrt{2}} [\sin \theta_e (1 + \eta \cos \theta_e) (\cos \phi^* \sin \theta^*)] H_- h_+ \right\}. \quad (2.31) \end{aligned}$$

The $H_{\pm}h_{\mp}$ terms are from transverse-longitudinal W -polarization interference. Notice that there is no transverse-transverse interference. This means the signs of H_{\pm} can be determined relative to h_{\mp} , but the overall sign is arbitrary. This equation simplifies somewhat if the daughter helicity-frame is chosen:

$$\begin{aligned} \frac{d\Gamma_{s'}}{dy d\Omega_e d\tilde{\Omega}_m} &= \frac{G_F^2 |V_{qq}|^2 KM^2y}{(4\pi)^5} \left[\frac{1}{2}(1 - \eta \cos \theta_e)^2 |H_+^{(s')}|^2 \right. \\ &\quad \left. + \frac{1}{2}(1 + \eta \cos \theta_e)^2 |H_-^{(s')}|^2 + \sin^2 \theta_e |H_0^{(s')}|^2 \right], \end{aligned} \quad (2.32)$$

where

$$H_{\pm}^{(s')} \equiv H_{\pm} \delta_{s'\pm}, \quad (2.33)$$

$$H_0^{(s')} \equiv h_{s'}. \quad (2.34)$$

Note that for daughter polarizations of $s' = +1(-1)$, the virtual- W is either longitudinally polarized or has transverse helicity components of $+1(-1)$. The longitudinal to transverse ratios are very process specific. Generally speaking, for decays in which the spectators are spin-singlets and the heavy quark carries the baryon spin, as in $\Lambda_b \rightarrow \Lambda_c e \nu$, positive daughter-helicity gives dominant transverse polarization of the virtual- W s while negative daughter-helicity gives dominant longitudinal- W polarization. The situation is quite different for decays in which the spectators are spin-triplets, as in $\Sigma_b \rightarrow \Sigma_c e \nu$, where longitudinal polarization always dominates. This will be made clear in the next section.

The spin independent rate is formed by summing over the final state helicity:

$$\begin{aligned} \frac{d\Gamma}{dy d\Omega_e d\tilde{\Omega}_m} &= \frac{G_F^2 |V_{qq}|^2 KM^2y}{(4\pi)^5} \left[\frac{1}{2}(1 - \eta \cos \theta_e)^2 |H_+|^2 \right. \\ &\quad \left. + \frac{1}{2}(1 + \eta \cos \theta_e)^2 |H_-|^2 + \sin^2 \theta_e |H_0|^2 \right], \end{aligned} \quad (2.35)$$

where

$$H_{\pm} \equiv \pm [aF_0 \mp gF_-], \quad (2.36)$$

$$H_0 \equiv \left\{ \left[2a \left(1 - \frac{1}{2}F_0 \right) - 2ka_+F_- \right]^2 + (2kg_+F_0 + gF_+)^2 \right\}^{1/2}. \quad (2.37)$$

The above helicity amplitudes should not be confused with the $H_{\pm,0}$ in Eq. (2.22), in which the spin-dependence (s 's) was suppressed for notational simplicity. Note especially that, when aF_0 and gF_- have the same relative sign, $|H_-| > |H_+|$. This is a reflection of the $V - A$ character at the quark level.

Besides examining just the angular distribution of the electron, it will be useful to integrate over all angles and consider only the momentum transfer distribution:

$$\frac{d\Gamma}{dy} = \frac{G_F^2 |V_{qQ}|^2 KM^2 y}{96\pi^3} (|H_+|^2 + |H_-|^2 + |H_0|^2). \quad (2.38)$$

It will be useful to define longitudinal and transverse rates, Γ_L and Γ_T , that involve only $|H_+|^2 + |H_-|^2$ and $|H_0|^2$ respectively. The labels “longitudinal” and “transverse” refer to the polarization of the virtual W . Γ_L is characterized by baryon spins (s 's) = $(\pm\mp)$ with a $\sin^2\theta_e$ electron distribution, while Γ_T is characterized by spins (s 's) = $(\pm\pm)$ and a $(1\mp\eta\cos\theta_e)^2$ electron distribution. Now all that remains is to calculate the Lorentz-invariant form factors in some model. This is addressed in the next section.

3. Form Factors

The basic idea is to use the nonrelativistic quark model to mock up the baryon states. The hadronic current is then calculated assuming the two light quarks are just spectators, so the weak hadronic current acts only on the heavy quarks with the usual $V - A$ form. The quark-model current is then compared with the parameterized current given by Eqs. (2.6) and (2.7) to obtain the form factors at maximum q^2 (in which the daughter is at rest frame in the parent rest-frame). A pole dominance model is then used to extend the q^2 behavior. This approach is taken in Ref. 4 and I adopt it here.

The vector and axial vector currents (2.6) and (2.7) are now evaluated in the parent rest frame. Since comparison with the quark-model currents will be made near maximum q^2 , the nonrelativistic form of the spinors is used and only leading order in the daughter momentum is kept. A short calculation gives:

$$\tilde{V}_{s's}^0 = \chi_{s'}^\dagger [\bar{g} + (M+m)\bar{g}_+ + (M-m)\bar{g}_-] \phi_s, \quad (3.1)$$

$$\tilde{V}_{s's} = \chi_{s'}^\dagger \left[\left(\frac{\bar{g}}{2m} + \bar{g}_+ - \bar{g}_- \right) \tilde{\mathbf{k}} + \frac{i\hat{\sigma} \times \tilde{\mathbf{k}}}{2m} \bar{g} \right] \phi_s, \quad (3.2)$$

$$\tilde{A}_{s's}^0 = \chi_{s'}^\dagger [\bar{a} - (M+m)\bar{a}_+ - (M-m)\bar{a}_-] \left(\frac{\hat{\sigma} \cdot \tilde{\mathbf{k}}}{2m} \right) \phi_s, \quad (3.3)$$

$$\tilde{\mathbf{A}}_{s's} = \chi_{s'}^\dagger [\bar{a}\hat{\sigma}] \phi_s. \quad (3.4)$$

Again, the tilde signifies the parent rest frame, ϕ_s and $\chi_{s'}$ are two component Pauli spinors for the parent and daughter baryon with spin along z and $\hat{\epsilon}$ respectively, and the bar over form factors means evaluation at maximum q^2 .

The current is now evaluated at the quark level. The parent baryon contains a heavy quark Q and two light quarks, which I simply refer to as u -quarks. Isospin and other flavor labels for the light di-quark system will usually be suppressed. The heavy quark has momentum \mathbf{p}_Q and the two lighter quarks have momentum \mathbf{p}_1 and \mathbf{p}_2 . While technically incorrect, a nonrelativistic approximation for the light di-quarks is reasonable since they are only spectators. The normalized parent baryon state vector is

$$\begin{aligned} |M(\mathbf{P}, s)\rangle = \sqrt{2M} \int d^3\mathbf{p}_{12} d^3\mathbf{l} \phi_M(\mathbf{p}_{12}, \mathbf{l}) \sum \chi_{s_1 s_2 s_Q}^s \\ \times |u(\mathbf{p}_1, s_1); u(\mathbf{p}_2, s_2); Q(\mathbf{p}_Q, s_Q)\rangle, \end{aligned} \quad (3.5)$$

where \mathbf{p}_{12} is the relative momentum of the two light quarks and \mathbf{l} is the relative momentum of Q and the light quark's center-of-mass, as shown in Fig. 3. The quark momenta in Eq. (3.5) are related to the integration variables and the baryon momentum by

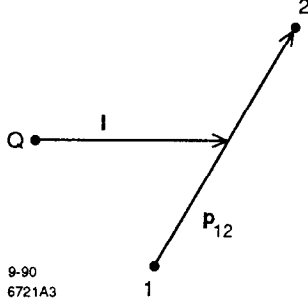


Fig. 3. Relative momenta of a three-quark system.

$$\mathbf{p}_Q = \frac{m_Q}{\tilde{M}} \mathbf{P} - \mathbf{l} , \quad (3.6)$$

$$\mathbf{p}_1 = \frac{m_1}{\tilde{M}} \mathbf{P} - \mathbf{p}_{12} + \frac{m_1}{m_{12}} \mathbf{l} , \quad (3.7)$$

$$\mathbf{p}_2 = \frac{m_2}{\tilde{M}} \mathbf{P} + \mathbf{p}_{12} - \frac{m_2}{m_{12}} \mathbf{l} , \quad (3.8)$$

where m_Q is the heavy quark mass, $m_{12} = m_1 + m_2$ is the sum of di-quark masses, and $\tilde{M} = m_Q + m_{12}$. It should be kept in mind that the baryon mass, M , and this “weak binding mass,” \tilde{M} , are not equal, although they are relatively close. It is also useful to invert the above equations:

$$\mathbf{P} = \mathbf{p}_1 + \mathbf{p}_2 + \mathbf{p}_Q , \quad (3.9)$$

$$\mathbf{p}_{12} = \frac{m_1}{m_{12}} \mathbf{p}_2 - \frac{m_2}{m_{12}} \mathbf{p}_1 , \quad (3.10)$$

$$\mathbf{l} = \frac{m_Q}{\tilde{M}} \mathbf{p}_1 + \frac{m_Q}{\tilde{M}} \mathbf{p}_2 - \frac{m_{12}}{\tilde{M}} \mathbf{p}_Q . \quad (3.11)$$

There are corresponding relations for the daughter baryon with the appropriate changes of mass and momentum. Also, the spin-sum in (3.5) has implicit flavor summation, which has been suppressed for notational simplicity. Since isospin symmetry is almost exact, Fermi-statistics requires the flavor-spin wave function to be symmetric in the u and d quarks (assuming relative S-wave spatial distributions and that only

overall color singlets are allowed). For the $\frac{1}{2}^+$ octet, I will assume slight $SU(3)$ flavor breaking. The two octets of mixed symmetry in the Clebsch-Gordan decomposition of $\mathbf{3} \times \mathbf{3} \times \mathbf{3} = \mathbf{10} + \mathbf{8}_S + \mathbf{8}_A + \mathbf{1}$, are combined with the corresponding spin-doublets of mixed symmetry in

$$\frac{\mathbf{1}}{2} \times \frac{\mathbf{1}}{2} \times \frac{\mathbf{1}}{2} = \frac{\mathbf{3}}{2} + \left(\frac{\mathbf{1}}{2}\right)_S + \left(\frac{\mathbf{1}}{2}\right)_A ,$$

to form the baryon flavor-spin wave function (the subscripts S and A refer to the symmetry of the two spectator quarks):

$$|B\rangle = \cos \theta_B \left| \mathbf{8}, \frac{1}{2} \right\rangle_S + \sin \theta_B \left| \mathbf{8}, \frac{1}{2} \right\rangle_A . \quad (3.12)$$

For exact $SU(3)$ flavor symmetry, the octet mixing angle $\theta_B = \pi/4$. I will be interested only in $B = \Lambda, \Sigma$ and Ξ . For bottom and charmed baryons ($Q = b$ or c), the wave functions are a little simpler. For isospin zero (Λ_Q), the spectators are spin-singlets, and for isospin one (Σ_Q), they are spin-triplets. For baryons with flavor ssQ , the s -quark spectators are spin-triplets. However, because of $SU(3)$ flavor breaking, the spectators in suQ may be spin-singlets (Ξ_Q) or spin-triplets (Ξ'_Q). Of course, the physical mass eigenstates are linear combinations of Ξ_Q and Ξ'_Q , but since they are in different spectator-quark spin representations, the mixing is small.¹⁶ I have omitted the charge labels, since in the spectator model all members of a given isomultiplet have the same amplitude. The bottom and charmed baryon states are, using an obvious short-hand mnemonic:

$$|\Lambda_Q, s\rangle = |ud_{[I=0]}; Q\rangle \chi_{(1)}^s , \quad (3.13)$$

$$|\Sigma_Q, s\rangle = |ud_{[I=1]}; Q\rangle \chi_{(3)}^s , \quad (3.14)$$

$$|\Omega_Q, s\rangle = |ss; Q\rangle \chi_{(3)}^s , \quad (3.15)$$

$$|\Xi_Q, s\rangle = |us; Q\rangle \chi_{(1)}^s , \quad (3.16)$$

$$|\Xi'_Q, s\rangle = |us; Q\rangle \chi_{(3)}^s , \quad (3.17)$$

where the singlet spin-state is

$$\chi_{(1)}^s = \begin{cases} \frac{1}{\sqrt{2}} [|+-+\rangle - |-++\rangle]; & s = +\frac{1}{2}, \\ \frac{1}{\sqrt{2}} [|+--\rangle - |-+-\rangle]; & s = -\frac{1}{2}, \end{cases} \quad (3.18)$$

and the triplet spin-state is

$$\chi_{(3)}^s = \begin{cases} -\frac{1}{\sqrt{6}} [|+-+\rangle + |-++\rangle - 2|++-\rangle]; & s = +\frac{1}{2}, \\ +\frac{1}{\sqrt{6}} [|+--\rangle + |-+-\rangle - 2|--+\rangle]; & s = -\frac{1}{2}, \end{cases} \quad (3.19)$$

with the ordering $|s_1 s_2 s_Q\rangle$. Note that $\chi_{(1)}^s$ and $\chi_{(3)}^s$ are symmetric and antisymmetric under spectator-quark interchanges, respectively.

To find the hadronic quark-model current, the current operator $J_{had}^\mu(0)$ is sandwiched between the parent state Eq. (3.5) and the corresponding daughter state. In the spectator model,

$$\langle q | J_{had}^\mu(0) | Q \rangle = \bar{q}(\mathbf{p}_q, s_q) \gamma^\mu (1 - \gamma_5) Q(\mathbf{p}_Q, s_Q). \quad (3.20)$$

The relative momentum variables of the daughter baryon will be denoted with primes, and momentum conservation of the spectator quarks in the parent rest frame gives

$$\tilde{\mathbf{p}}'_{12} = \tilde{\mathbf{p}}_{12}, \quad (3.21)$$

$$\tilde{\mathbf{l}}' = \tilde{\mathbf{l}} - \frac{m_{12}}{\tilde{m}} \tilde{\mathbf{k}}, \quad (3.22)$$

and

$$\tilde{\mathbf{p}}_Q = -\tilde{\mathbf{l}}, \quad (3.23)$$

$$\tilde{\mathbf{p}}_q = \tilde{\mathbf{k}} - \tilde{\mathbf{l}}. \quad (3.24)$$

The hadronic matrix element becomes (I have dropped the tilde from the integration variables):

$$\begin{aligned}
H^{(s's) \mu} &= \langle m, s' | J_{had}^\mu(0) | M, s \rangle \\
&= \sqrt{4Mm} \left(\frac{m_q}{\tilde{m}} \right)^3 \int d^3 \mathbf{p}_{12} d^3 \mathbf{l} \phi_m^*(\mathbf{p}'_{12}, \mathbf{l}') \phi_M(\mathbf{p}_{12}, \mathbf{l}) \langle s' | J^\mu | s \rangle, \quad (3.25)
\end{aligned}$$

where

$$\langle s' | J^\mu | s \rangle \equiv \sum \chi_{s_1 s_2 s_q}^{s'} \chi_{s_1 s_2 s_Q}^s \bar{q}(\tilde{\mathbf{p}}_q, s_q) \gamma^\mu (1 - \gamma_5) Q(\tilde{\mathbf{p}}_Q, s_Q). \quad (3.26)$$

In the derivation of Eqs. (3.25) and (3.26), the di-quark spectators give delta functions of quark momenta, and the $(m_q/\tilde{m})^3$ factor is simply the Jacobian that converts an integration over the relative momenta \mathbf{p}'_{12} and \mathbf{l}' to an integration over di-quark momenta for the daughter baryon. In the approximations below I drop the $(m_{12}/\tilde{m})\tilde{\mathbf{k}}$ term in Eq. (3.22), and this induces an ambiguity in this Jacobian factor. If the relative momenta of the daughter were integrated over in Eq. (3.25), rather than the parent, there would be a factor of $(m_q/\tilde{M})^3$ instead. In the spectator model the di-quark masses should not effect the rate, so I take them light enough to neglect these factors. This can be better justified by considering an elastic vector interaction, such as electromagnetism. The Ward identity gives the correct normalization of the vector form factor at zero recoil. Considering a baryon with only one electrically charged heavy quark and using the state normalization given in Eq. (3.5), the form factor normalization must be $g(y_{max}) = \sqrt{4Mm}$, and the $(m_q/\tilde{m})^3$ factor should in fact be dropped, and I adopt the same prescription for weak transition currents below.

To find the quark-model currents, I use the nonrelativistic form of the spinors in Eq. (3.26), keeping terms linear in momentum, and then substitute this into Eq. (3.25). I drop terms proportional to m_{12}/\tilde{m} in the argument of ϕ_m^* , and assume flavor independence, $\phi_m = \phi_M = \phi$. By parity, the terms linear in \mathbf{l} integrate to zero, giving

TABLE I

Spin and flavor factors.

Process	ξ	N_{mM}
$\Lambda_Q \rightarrow \Lambda_q e \nu$	1	1
$\Sigma_Q \rightarrow \Sigma_q e \nu$	-1/3	1
$\Omega_Q \rightarrow \Omega_q e \nu$	-1/3	1
$\Xi_Q \rightarrow \Xi_q e \nu$	1	1
$\Xi'_Q \rightarrow \Xi'_q e \nu$	-1/3	1
$\Lambda_Q \rightarrow \Lambda e \nu$	1	$\sqrt{\frac{2}{3}} \sin \theta_\Lambda$
$\Sigma_Q \rightarrow \Sigma e \nu$	-1/3	$\sqrt{\frac{2}{3}} \cos \theta_\Sigma$
$\Xi_Q \rightarrow \Xi e \nu$	1	$\frac{1}{\sqrt{2}} \sin \theta_\Xi$
$\Xi'_Q \rightarrow \Xi e \nu$	-1/3	$\frac{1}{\sqrt{6}} \cos \theta_{\Xi'}$

$$\tilde{V}_{s's}^0 = \sqrt{4Mm} \langle \chi_{s'}^\dagger \phi_s \rangle, \quad (3.27)$$

$$\tilde{\mathbf{V}}_{s's} = \sqrt{4Mm} \left\langle \chi_{s'}^\dagger \left[\frac{\tilde{\mathbf{k}} + i\hat{\sigma} \times \tilde{\mathbf{k}}}{2m_q} \right] \phi_s \right\rangle, \quad (3.28)$$

$$\tilde{A}_{s's}^0 = \sqrt{4Mm} \left\langle \chi_{s'}^\dagger \left[\frac{\hat{\sigma} \cdot \tilde{\mathbf{k}}}{2m_q} \right] \phi_s \right\rangle, \quad (3.29)$$

$$\tilde{\mathbf{A}}_{s's} = \sqrt{4Mm} \langle \chi_{s'}^\dagger \hat{\sigma} \phi_s \rangle, \quad (3.30)$$

where I have used the shorthand notation

$$\langle \Gamma_{s's} \rangle \equiv \sum \chi_{s_1 s_2 s_q}^{s'} \chi_{s_1 s_2 s_Q}^s \Gamma_{(s_q s_Q)}. \quad (3.31)$$

The only thing left to do now is choose particular baryons, evaluate Eqs. (3.27)–(3.30), and then make comparisons with Eqs. (3.1)–(3.4) for various spin choices.

Ignoring flavor for the moment and using Eqs. (3.18) and (3.19), one can show $\langle \chi_{s'}^\dagger, \hat{\sigma} \phi_s \rangle = \chi_{s'}^\dagger [\xi \hat{\sigma}] \phi_s$, where $\xi = 1$ when the spectators are spin-singlets and $\xi = -1/3$ when they are spin-triplets. When flavor is considered, a factor N_{mM} given in Table I, comes from Eq. (3.12) and the explicit octet flavor states of mixed symmetry. For the baryons considered in this paper, Eqs. (3.27)–(3.30) take the form

$$\tilde{V}_{s's}^0 = \sqrt{4Mm} N_{mM} \chi_{s'}^\dagger \phi_s, \quad (3.32)$$

$$\tilde{V}_{s's} = \sqrt{4Mm} N_{mM} \chi_{s'}^\dagger \left[\frac{\tilde{\mathbf{k}} + i\xi \hat{\sigma} \times \tilde{\mathbf{k}}}{2m_q} \right] \phi_s, \quad (3.33)$$

$$\tilde{A}_{s's}^0 = \sqrt{4Mm} N_{mM} \chi_{s'}^\dagger \xi \left[\frac{\hat{\sigma} \cdot \tilde{\mathbf{k}}}{2m_q} \right] \phi_s, \quad (3.34)$$

$$\tilde{\mathbf{A}}_{s's} = \sqrt{4Mm} N_{mM} \chi_{s'}^\dagger [\xi \hat{\sigma}] \phi_s, \quad (3.35)$$

where $\xi = 1$ if the parent/daughter di-quarks are spin singlets and $\xi = -1/3$ if they are spin triplets (there are no singlet to triplet transitions in the spectator model).

Comparing Eqs. (3.32)–(3.35) with Eqs. (3.1)–(3.4) gives the following set of equations for the form factors at maximum q^2 :

$$\bar{g} + (M + m)\bar{g}_+ + (M - m)\bar{g}_- = \sqrt{4Mm} N_{mM}, \quad (3.36)$$

$$\frac{\bar{g}}{2m} + \bar{g}_+ - \bar{g}_- = \frac{\sqrt{Mm}}{m_q} N_{mM}, \quad (3.37)$$

$$\bar{g} = \sqrt{4Mm} \frac{m}{m_q} \xi N_{mM}, \quad (3.38)$$

$$\bar{a} - (M + m)\bar{a}_+ - (M - m)\bar{a}_- = \sqrt{4Mm} \frac{m}{m_q} \xi N_{mM}, \quad (3.39)$$

$$\bar{a} = \sqrt{4Mm} \xi N_{mM}. \quad (3.40)$$

For the axial-vector form factors, there are two equations in three unknowns, so unfortunately they are not completely determined; I will take \bar{a}_+ as a free parameter. Note from Eq. (2.36) that H_\pm are independent of a_+ , so the transverse rate,

characterized by baryon spins $(s's) = (\pm\pm)$ and a $(1 \mp \eta \cos \theta_e)^2$ electron distribution, can be predicted with no fitting to data. Solving the above equations for the vector form factors \bar{g}_\pm gives

$$\bar{g}_\pm = -\sqrt{\frac{m}{M}} N_{mM} \left[\left(\xi \frac{m}{m_q} - 1 \right) + \frac{m \mp M}{2m_q} (1 - \xi) \right], \quad (3.41)$$

while (3.39) and (3.40) give the constraint equation

$$(M + m)\bar{a}_+ + (M - m)\bar{a}_- = -\sqrt{4Mm} \left(\frac{m}{m_q} - 1 \right) \xi N_{mM}. \quad (3.42)$$

Ref. 16 derives form factor constraints in the infinite quark-mass limit. In this limit a new heavy-quark flavor symmetry emerges since the long wave length properties of the light quarks become independent of the heavy quark mass. For decays in which $\xi = 1$, as in $\Lambda_b \rightarrow \Lambda_c e \nu$, Ref. 16 shows the amplitude is determined by one universal form factor—in the notation of this paper, $g = a$, $g_\pm = 0$ and $a_\pm = 0$. In the infinite quark-mass limit, in which $m/m_q \rightarrow 1$, Eqs. (3.38) and (3.40) give the first of these relations ($g = a$) and Eq. (3.41) gives the second ($g_\pm = 0$). Actually, the results of Ref. 16 are reproduced only at the end point, and a pole dominance assumption gives an extrapolation to arbitrary q^2 . While Eq. (3.42) does not alone imply $a_\pm = 0$ in the infinite quark-mass limit, it is consistent with this, which suggests that smaller values of \bar{a}_+ should be preferred for decays in which $\xi = 1$. Ref. 16 derives somewhat weaker constraints for decays in which $\xi = -1/3$, as in $\Omega_b \rightarrow \Omega_c e \nu$. In the notation of this paper, the relations (45) and (48) of Ref. 16 become $(M + m)\bar{a}_+ + (M - m)\bar{a}_- = 0$ and $(M - m)\bar{g}_+ + (M - m)\bar{g}_- = 0$,¹⁷ and in the infinite quark-mass limit Eqs. (3.42) and (3.36) reduce to these constraints. Unlike the $\xi = 1$ case, the vector form factors \bar{g}_\pm are no longer small; however, small values of the axial form factors \bar{a}_\pm are allowed since the right hand side of Eq. (3.42) vanishes in the infinite quark-mass limit. Unfortunately, Ref. 16 gives no indication of the preferred \bar{a}_\pm values as it did for Λ_Q and Ξ_Q decays. However, another constraint equation for \bar{a}_\pm

may be found by extending the calculation that leads up to Eq. (3.42) to second order in $\tilde{\mathbf{k}}$.¹⁸ Including the next-to-leading order terms in $\tilde{\mathbf{k}}$, the axial three-vector current (3.4) becomes:

$$\tilde{\mathbf{A}}_{s's} = \chi_{s'}^\dagger \left[\left(1 + \frac{\tilde{\mathbf{k}}^2}{8m^2} \right) a \hat{\sigma} - [\bar{a}_+ - \bar{a}_-] \left(\frac{\hat{\sigma} \cdot \tilde{\mathbf{k}}}{2m} \right) \tilde{\mathbf{k}} \right] \phi_s . \quad (3.43)$$

The form factor a , above, is not yet evaluated at maximum q^2 . The current must now be calculated at the quark level. As in deriving Eq. (3.35), the terms of order m_{12}/\tilde{m} and l^2 will be dropped. The terms linear in l again integrate to zero and the quark-model calculation, in next to leading order, gives:

$$\tilde{\mathbf{A}}_{s's} = \sqrt{4Mm} N_{mM} \chi_{s'}^\dagger \left[\xi \left(1 + \frac{\tilde{\mathbf{k}}^2}{8m_q^2} \right) \hat{\sigma} \right] \phi_s . \quad (3.44)$$

Comparing Eqs. (3.43) and (3.44) for $s's = \pm\mp$ (longitudinal virtual W s) gives:

$$\left(1 + \frac{\tilde{\mathbf{k}}^2}{8m^2} \right) a = \sqrt{4Mm} N_{mM} \xi \left(1 + \frac{\tilde{\mathbf{k}}^2}{8m_q^2} \right) . \quad (3.45)$$

This just gives a negligible $\tilde{\mathbf{k}} \neq 0$ correction to a . Next, making the comparison for $s's = \pm\pm$ (transverse virtual W s) and using Eq. (3.45), a new constraint equation is found:

$$\bar{a}_+ - \bar{a}_- = 0 . \quad (3.46)$$

It should be emphasized that Eq. (3.46) only represents a best guess, since in going to second order in the daughter momentum there are relativistic corrections I have ignored.

Finally, using Eqs. (3.42) and (3.46),

$$\bar{a}_\pm = -\sqrt{\frac{m}{M}} \left(\frac{m}{m_q} - 1 \right) \xi N_{mM} . \quad (3.47)$$

Note that in the infinite quark-mass limit, this second order calculation gives $a_\pm = 0$. This is in agreement with Ref. 16 for decays in which $\xi = 1$. Furthermore, this result

suggests that a_{\pm} remain small even for decays in which $\xi \neq 1$, although g_{\pm} may become large for such decays.

In summary, the form factors at the maximum q^2 end-point are:

$$\bar{g} = \sqrt{4Mm} \frac{m}{m_q} \xi N_{mM} , \quad (3.48)$$

$$\bar{a} = \sqrt{4Mm} \xi N_{mM} , \quad (3.49)$$

$$\bar{g}_{\pm} = -\sqrt{\frac{m}{M}} N_{mM} \left[\left(\xi \frac{m}{m_q} - 1 \right) + \frac{m \mp M}{2m_q} (1 - \xi) \right] , \quad (3.50)$$

$$\bar{a}_{\pm} = -\sqrt{\frac{m}{M}} \left(\frac{m}{m_q} - 1 \right) \xi N_{mM} . \quad (3.51)$$

Again it should be emphasized that Eq. (3.51) represents only a best guess, and I will at times continue to keep \bar{a}_+ a free parameter. Also, recall that none of these caveats apply for transverse- W rates, which are independent of \bar{a}_+ .

Now, to extend the q^2 behavior beyond the end point, a pole dominance model is assumed. The g form factor, for example, scales as

$$g(y) = \frac{y_{max} - y_{res}}{y - y_{res}} \bar{g} , \quad (3.52)$$

where $y_{max} = (1 - m/M)^2$ and $y_{res} = (m_{qQ}^*/M)^2$, with m_{qQ}^* being the mass of the first excited Qq -vector meson resonance above the parent baryon mass. For simplicity, I assume all the form factors scale using the same resonance mass. This is a practical assumption, since the masses of such resonances are not measured well enough to distinguish their parity and charge conjugation.

4. Model Results

This section gives numerical results for various exclusive decay modes. For the process $\Lambda_b^0 \rightarrow \Lambda_c^+ e^- \bar{\nu}_e$, I take the mass of Λ_c to be $m = 2.28$ GeV, the appropriate KM-matrix element $V_{bc} = 0.046$, and the charmed quark mass $m_c = 1.8$ GeV. The masses of Λ_b and the $b\bar{c}$ -vector resonance used for the pole-dominance model are uncertain. I take $M = 5.5$ GeV and a pole mass $m^* = 6.0$ GeV as ball-park figures. The rates are rather insensitive to the exact pole mass, and a variation in m^* of about 5% gives a variation in the rates of typically 5%–10%. Of course the absolute rates are very sensitive to the value of the parent-baryon mass since (2.38) is proportional to $M^4 m$. When M is better known, one can simply rescale the rates found below by $(M_{better}/M_{old})^4$, to an accuracy of about 10%. The form factors at maximum q^2 are $\bar{g} = 9.00$ GeV, $\bar{a} = 7.09$ GeV and $\bar{g}_+ = -0.174$. For $\bar{a}_+ = 0$, the exclusive rate and the longitudinal- to transverse- W ratio is $\Gamma(\Lambda_b \rightarrow \Lambda_c e \nu) = 5.7 \times 10^{10} \text{ sec}^{-1}$ and $\Gamma_L/\Gamma_T = 1.1$. Figs. 4–5 show the rate and the longitudinal to transverse ratio as a function of \bar{a}_+ . Note that for values of \bar{a}_+ close to zero, there are approximately equal mixtures of transverse- and longitudinal- W polarization. The total exclusive rate, along with the longitudinal and transverse rates, across the Dalitz plot are shown in Fig. 6 for $\bar{a}_+ = -0.17$ (the second order prediction). The transverse rate is independent of \bar{a}_+ , and Fig. 7 illustrates the sensitivity of the longitudinal width across the Dalitz plot for a range of \bar{a}_+ . Note that the sensitivity is greatest for lower values of $y = q^2/M^2$. This is because the kinematic factor K in Eq. (2.15) vanishes at maximum q^2 , which washes out all dependence on \bar{a}_+ .

Tables II and III contain a summary of other processes. The rates presented there use the order- \tilde{k}^2 calculation for \bar{a}_+ . There are two qualitatively different cases: when the spectators are spin-singlets ($\xi = 1$) and when they are spin-triplets ($\xi = -1/3$). Figs. 4–15 summarize the exclusive rates, longitudinal to transverse ratios and Dalitz plot behavior for two representative decays, $\Lambda_b \rightarrow \Lambda_c e \nu$ and $\Omega_b \rightarrow \Omega_c e \nu$. Other decays are qualitatively similar to one of the previous two, depending on the spin of the spectators.

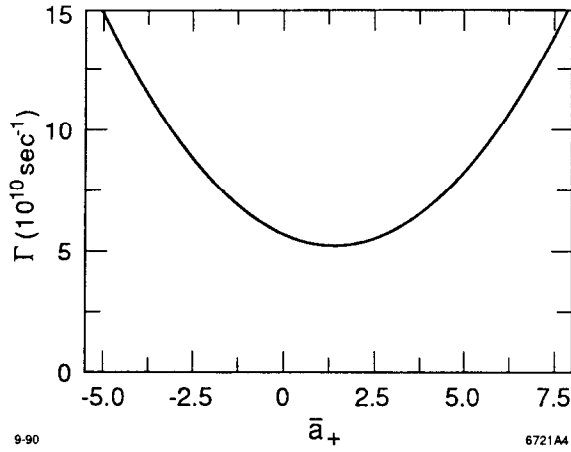


Fig. 4. Rate for $\Lambda_b \rightarrow \Lambda_c e \nu$.

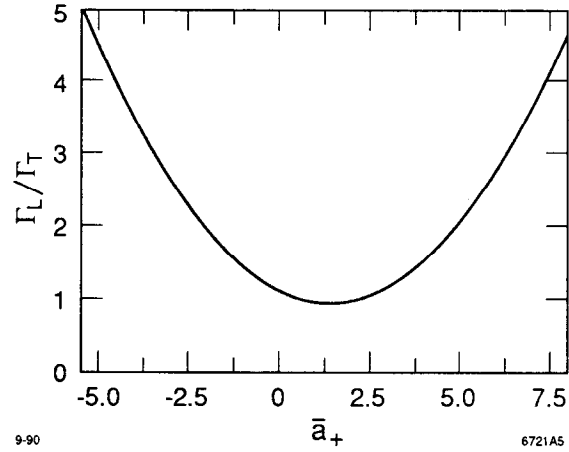


Fig. 5. Longitudinal- to transverse- W ratio for $\Lambda_b \rightarrow \Lambda_c e \nu$.

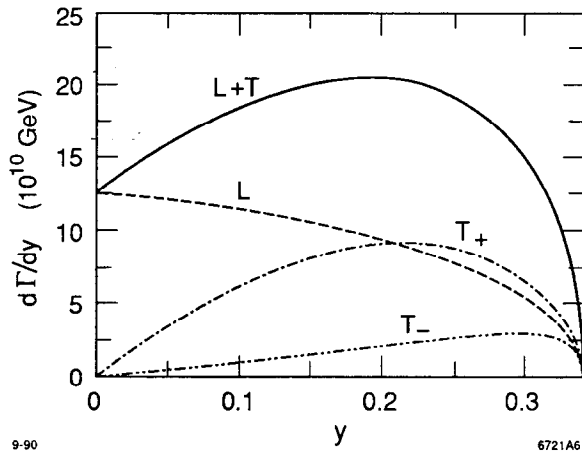


Fig. 6. Total exclusive rate along with longitudinal- and transverse- W rates for $\Lambda_b \rightarrow \Lambda_c e \nu$. The T_{\pm} signify $\pm W$ -helicity, and the second order prediction of $\bar{a}_+ = -0.17$ was used.

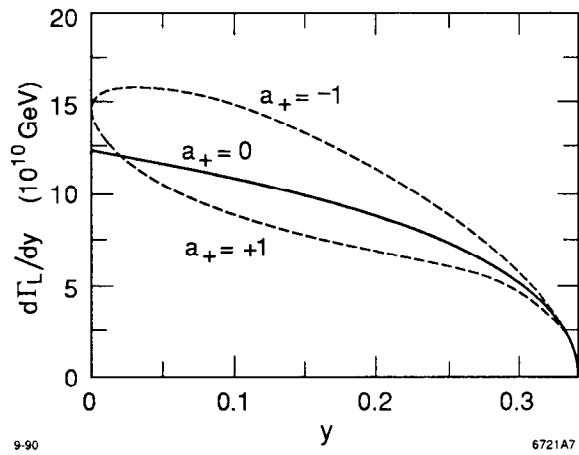


Fig. 7. Longitudinal rate sensitivity upon \bar{a}_+ for $\Lambda_b \rightarrow \Lambda_c e \nu$.

TABLE II

Kinematic Parameters. The * above a mass indicates large experimental uncertainty.

Process	M (GeV)	m (GeV)	m_q (GeV)	m^*	V_{qq}
$\Lambda_b \rightarrow \Lambda_c e \nu$	5.5*	2.28	1.8	6.0*	0.046
$\Sigma_b \rightarrow \Sigma_c e \nu$	5.8*	2.45	1.8	6.0*	0.046
$\Omega_b \rightarrow \Omega_c e \nu$	6.1*	2.7	1.8	6.4*	0.046
$\Xi_b \rightarrow \Xi_c e \nu$	5.8*	2.46	1.8	6.0*	0.046
$\Lambda_c \rightarrow \Lambda e \nu$	2.28	1.12	0.51	2.5*	0.975
$\Sigma_c \rightarrow \Sigma e \nu$	2.45	1.19	0.51	2.8*	0.975
$\Xi_c \rightarrow \Xi e \nu$	2.46	1.31	0.51	2.8*	0.975

TABLE III

Form Factors and Rates. The value of \bar{a}_+ is the second order $\tilde{\mathbf{k}}$ prediction.

Process	\bar{a}_+	\bar{g} (GeV)	\bar{a} (GeV)	\bar{g}_+	Γ (10^{10} sec^{-1})	Γ_T (10^{10} sec^{-1})	Γ_L/Γ_T
$\Lambda_b \rightarrow \Lambda_c e \nu$	-0.17	9.0	7.1	-0.17	5.9	2.7	1.2
$\Sigma_b \rightarrow \Sigma_c e \nu$	0.079	-3.4	-2.5	1.8	4.3	0.37	10.7
$\Omega_b \rightarrow \Omega_c e \nu$	0.11	-4.1	-2.7	1.8	5.4	0.44	11.2
$\Xi_b \rightarrow \Xi_c e \nu$	-0.24	10.3	7.6	-0.24	7.2	3.3	1.2
$\Lambda_c \rightarrow \Lambda e \nu$	-0.48	4.0	1.8	-0.48	9.8	3.8	1.6
$\Sigma_c \rightarrow \Sigma e \nu$	0.18	-1.5	-0.66	1.38	10.2	0.65	14.8
$\Xi_c \rightarrow \Xi e \nu$	-0.58	4.6	1.8	-0.58	8.5	3.1	1.7

Note that for baryons whose spin is carried by the heavy quark ($\xi = 1$), the longitudinal polarization is from one to two times greater than the transverse polarization—with bottom baryons tending to equal longitudinal and transverse mixtures and charmed baryons tending to predominately longitudinal mixtures. When the spectators are in a spin triplet, as in Ω_q , the longitudinal polarization dominates by at least a factor of 10!

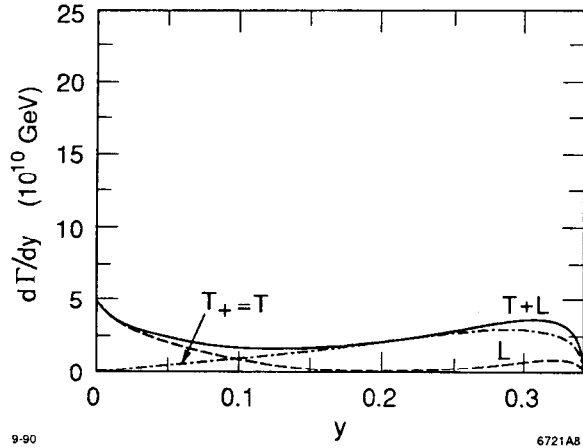


Fig. 8. Total exclusive rate along with longitudinal- and transverse- W rates for $\Lambda_b \rightarrow \Lambda_c e \nu$ with a + polarized daughter. The T_{\pm} signify $\pm W$ -helicity, and the second order prediction of $\bar{a}_+ = -0.17$ was used. In this and the following figure, T_+ is given by a dash-dotted line and T_- by a dash-double-dotted line.

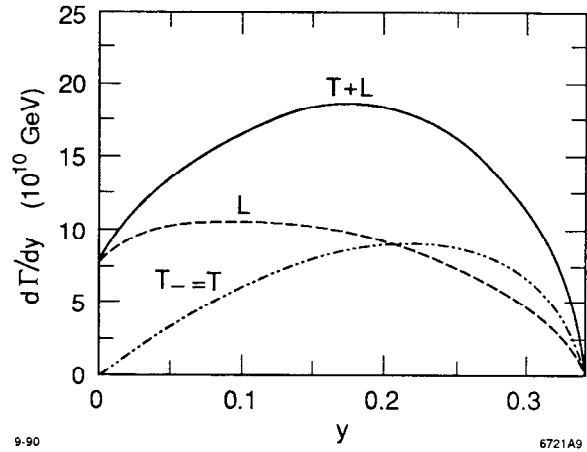


Fig. 9. Same as above, but for a daughter of polarization $s' = -$.

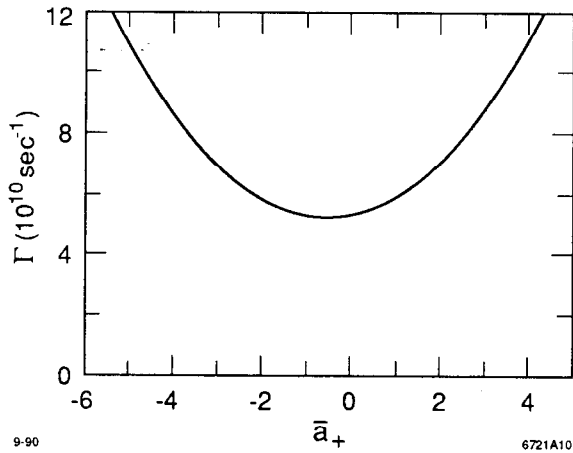


Fig. 10. Rate for $\Omega_b \rightarrow \Omega_c e \nu$.

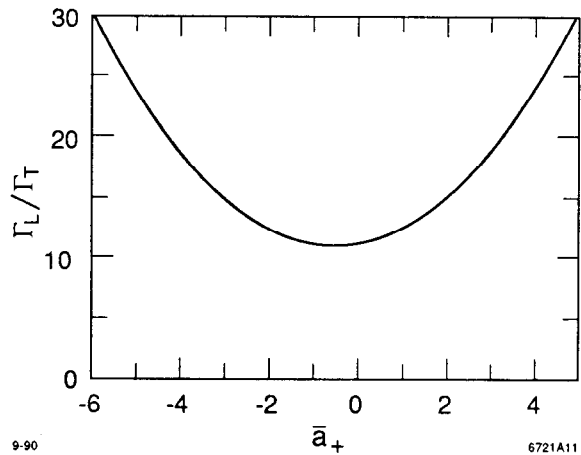


Fig. 11. Longitudinal- to transverse- W ratio for $\Omega_b \rightarrow \Omega_c e \nu$.

Figs. 8–9 examine the Dalitz plot behavior of $\Lambda_b \rightarrow \Lambda_c e \nu$, for positively and negatively polarized daughters respectively. For $s' = +$, the W -polarization is mainly transverse; and for $s' = -$, there is about an equal longitudinal and transverse mixture. The situation for $\Omega_b \rightarrow \Omega_c e \nu$ is shown in Figs. 14–15. In this case, the virtual

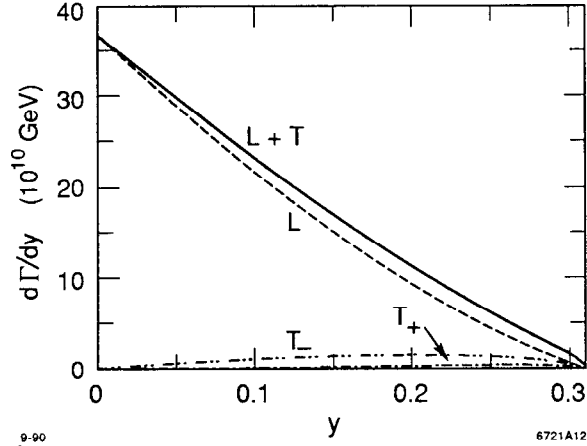


Fig. 12. Total exclusive rate along with longitudinal- and transverse- W rates for $\Omega_b \rightarrow \Omega_c e \nu$. The T_{\pm} signify $\pm W$ -helicity, and the second order prediction of $\bar{a}_+ = -0.08$ was used.

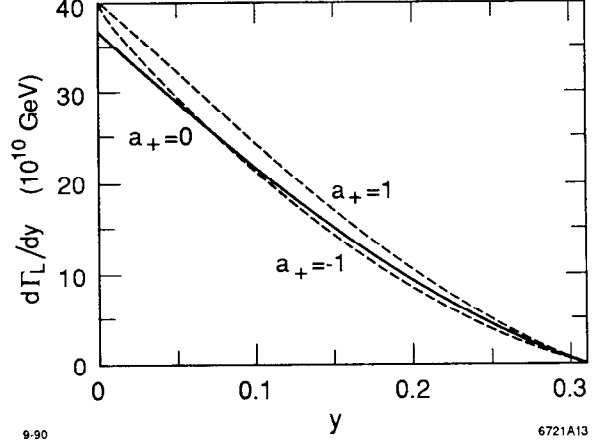


Fig. 13. Longitudinal rate sensitivity upon \bar{a}_+ for $\Omega_b \rightarrow \Omega_c e \nu$.

TABLE IV

Exclusive rates and longitudinal to transverse ratio for polarized daughter baryons.

Process	Daughter Hel. $s' = +$			Daughter Hel. $s' = -$		
	Γ (10^{10} sec^{-1})	Γ_T (10^{10} sec^{-1})	Γ_L/Γ_T	Γ (10^{10} sec^{-1})	Γ_T (10^{10} sec^{-1})	Γ_L/Γ_T
$\Lambda_b \rightarrow \Lambda_c e \nu$	0.85	0.55	0.56	5.0	2.2	1.3
$\Sigma_b \rightarrow \Sigma_c e \nu$	2.7	0.07	36.8	1.6	0.30	4.5
$\Omega_b \rightarrow \Omega_c e \nu$	3.4	0.08	41.2	2.0	0.36	4.6
$\Xi_b \rightarrow \Xi_c e \nu$	0.99	0.63	0.57	6.2	2.7	1.4
$\Lambda_c \rightarrow \Lambda e \nu$	0.85	0.45	0.87	9.0	3.4	1.7
$\Sigma_c \rightarrow \Sigma e \nu$	6.5	0.07	97.2	3.7	0.58	5.4
$\Xi_c \rightarrow \Xi e \nu$	0.67	0.34	0.93	7.8	2.8	1.8

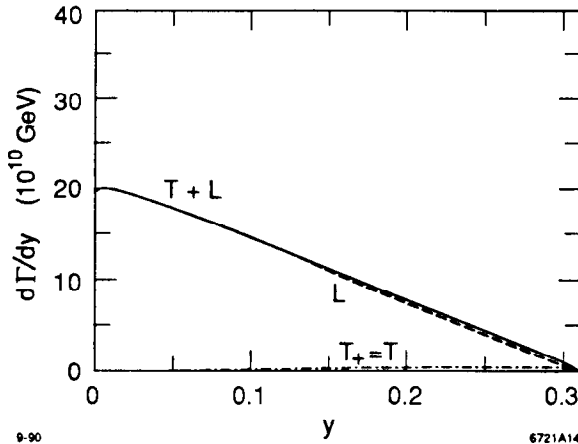


Fig. 14. Total exclusive rate along with longitudinal- and transverse- W rates for $\Omega_b \rightarrow \Omega_c e \nu$ with a $+$ polarized daughter. The T_{\pm} signify $\pm W$ -helicity, and the second order prediction of $\bar{a}_+ = -0.08$, was used. In this and the following figure, T_+ is given by a dash-dotted line and T_- by a dash-double-dotted line.

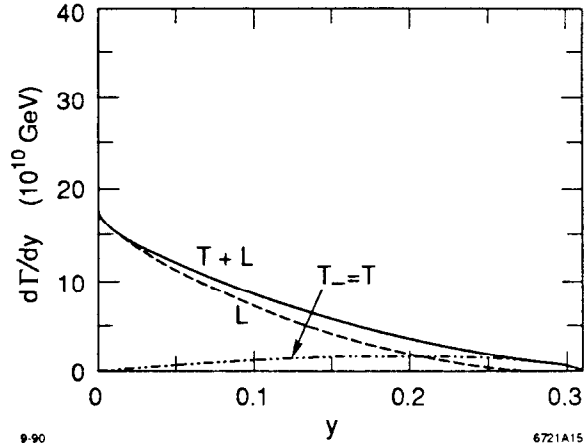


Fig. 15. Same as above but for a daughter of polarization $s' = -$.

W is predominately longitudinal, but much more so for positive helicity daughters. In both cases, $s' = +$ ($s' = -$) polarized daughters are never seen with negative (positive) helicity W s. Table IV gives a summary of other processes for polarized daughter states. The two processes represented in the figures are the most experimentally relevant. For example, the splitting between Σ_b and Λ_b is probably greater than a pion mass, so semileptonic Σ_b decay has much too small a branching ratio to be measured. The Ω_b and Ω_c , on the other hand, are stable to strong decays, and there is a good chance of observing their semileptonic modes and comparing to theory

ACKNOWLEDGMENTS

I would like to thank J. Bjorken and I. Dunietz for many useful discussions and suggestions.

REFERENCES

- ¹G. Altarelli *et al.*, Nucl. Phys. **B208**, 365 (1982).
- ²B. Grinstein, N. Isgur, and M. B. Wise, Phys. Rev. Lett. **56**, 298 (1986); Caltech Report CALT-68-1311 (1986); B. Grinstein, N. Isgur, D. Scora, and M. B. Wise, Phys. Rev. **D39**, 799 (1989).
- ³M. Bauer, B. Stech, and M. Wirbel, Z. Phys. **C29**, 637 (1985).
- ⁴T. Altomari and L. Wolfenstein, Phys. Rev. Lett. **58**, 1583 (1987); Phys. Rev. **D37**, 681 (1988).
- ⁵J. G. Korner and G. A. Schuler, Z. Phys. **C38**, 511 (1988).
- ⁶J. C. Anjos *et al.*, Phys. Rev. Lett. **62**, 722 (1989). The Mark III result for the decay width is consistent with E691: J. M. Izen, SLAC-PUB-4753 (1988).
- ⁷M. Bauer and M. Wirbel, Z. Phys. **C42**, 671 (1989).
- ⁸E. Golowich *et al.*, Phys. Lett. **B213**, 521 (1988).
- ⁹N. Isgur and D. Scora, Phys. Rev. **D40**, 1491 (1989).
- ¹⁰F. J. Gilman and R. L. Singleton Jr., Phys. Rev. **D41**, 142 (1990)
- ¹¹J. G. Korner and G. A. Schuler, Mainz Report MZ-TH/88-14 (1988); Phys. Lett. **B226**, 185 (1989).
- ¹²K. Hagiwara, A. D. Martin, and M. F. Wade, Phys. Lett. **B228**, 144 (1989).
- ¹³The daughter helicity frame has $-x$ polar and y and $-z$ axes as a coordinate frame, and the usual polar and azimuthal angles θ and ϕ are related to θ^* and ϕ^* by $\theta = \pi + \theta^*$ and $\phi = -\phi^*$.
- ¹⁴J. Bjorken and S. Drell, *Relativistic Quantum Mechanics*, Vol. I.

¹⁵I use the following conventions for Pauli-spinors along a direction \hat{e} , defined by azimuthal and polar angles θ and ϕ :

$$\chi_+ = \begin{pmatrix} e^{-i\phi/2} \cos \theta/2 \\ e^{i\phi/2} \sin \theta/2 \end{pmatrix},$$

and

$$\chi_- = \begin{pmatrix} -e^{-i\phi/2} \sin \theta/2 \\ e^{i\phi/2} \cos \theta/2 \end{pmatrix}.$$

The daughter helicity-frame angles θ^* and ϕ^* , given by $\theta = \pi + \theta^*$ and $\phi = -\phi^*$, should then be used in the above spinors.

¹⁶N. Isgur and M. Wise, Univ. of Toronto Report UTPT-90-03 (1990).

¹⁷The relations between the form factors used here and those in Ref. 16 are: $g_{\pm} = \frac{F_2}{2M} \pm \frac{F_3}{2m}$, $a_{\pm} = \frac{G_2}{2M} \pm \frac{G_3}{2m}$, $g = F_1$ and $a = G_1$.

¹⁸T. Altomari and L. Wolfenstein, Carnegie Mellon University Report CMU-HEP-86-17 (1986).